No-Reference Quality Assessment of Contrast-Distorted Images using Contrast Enhancement

Jia Yan, Jie Li, Xin Fu

Abstract:

No-reference image quality assessment (NR-IQA) aims to measure the image quality without reference image. However, contrast distortion has been overlooked in the current research of NR-IQA. In this paper, we propose a very simple but effective metric for predicting quality of contrast-altered images based on the fact that a high-contrast image is often more similar to its contrast enhanced image. Specifically, we first generate an enhanced image through histogram equalization. We then calculate the similarity of the original image and the enhanced one by using structural-similarity index (SSIM) as the first feature. Further, we calculate the histogram based entropy and cross entropy between the original image and the enhanced one respectively, to gain a sum of 4 features. Finally, we learn a regression module to fuse the aforementioned 5 features for inferring the quality score. Experiments on four publicly available databases validate the superiority and efficiency of the proposed technique.

Keywords: contrast distortion, no-reference image quality assessment, histogram equalization, similarity measurement, support vector regression

1. Introduction

As the users' requirements for high-quality images are increasingly rising, no-reference image quality assessment (NR-IQA) has recently become an active research topic, whose objective is to estimate the human perception of image quality without any access to the original reference image [1, 2]. It can be deployed in every location of an image communication system whenever the distorted image is available for evaluation.

The majority of current NR-IQA methods are proposed based on two steps, namely, feature extraction and SVR-based regression module. Natural scene statistics (NSS) based features constitute the majority of existing NR-IQA methods. A plethora of NSS models in different spatial or transform domains have been incorporated into state-of-the-art methods [3-12]. In [12], a bag of feature maps over several transform domains and three color spaces are used, which can be seemed as a combination of the previous methods. Further, a growing body of researchers turn to resorting to advanced neural networks and learning systems, e.g., deep belief net [13, 14], shallow Convolutional Neural Networks (CNN) [15, 16] and deep CNNs [17].

However, traditional NR-IQA studies are mainly devoted to gauging commonly encountered artifacts, for example, Gaussian blur, noise, and compression. In comparison, little investigation is dedicated to the issue of NR-IQA for evaluation of the contrast-changed images. It is worth noting that contrast distortion is often introduced during the image acquisition due to limitation of the acquisition device or poor lighting condition. Moreover, while the aforementioned NR-IQA methods work quite well on commonly seen distortions, they always perform ineffectively on contrast distortion [9], as will

also be shown later in this paper. As a matter of fact, IQA of contrast-distorted images is an important research topic, which can be used as a guider or evaluation criteria in contrast enhancement technologies [18, 19].

Currently, there are several studies only focusing on contrast distorted images. Gu et al. [19, 20] first systematically studied this issue; and designed the CID2013 and CCID2014 databases dedicated to image contrast change, and meanwhile proposed reduced reference IQA (RR-IQA) techniques based on phase congruency and information statistics of the image histogram. Liu et al. [21] also proposed a RR-IQA metric RCIQM with the integration of free energy theory and the histogram comparison of the contrast-altered image with that of the reference image. But these methods rely on partial access to the reference image, and therefore, NR algorithms are eagerly required. Fang et al. [22] proposed a NR quality metric based on the NSS regulation including the moment and entropy features, and it achieves better results than the general-purpose NSS based methods. Gu et al. [23] proposed a training-free blind quality method NIQMC based on the concept of information maximization by computing entropy of particular areas and also comparing the image histogram with the uniformly distributed histogram. Gu et al. [24] lately extracted 17 features based on contrast, sharpness, brightness and more, and then yields an IQA metric BIQME using a regression module, which is learned with gathered big-data training samples.

In this paper, we develop a simple yet effective NR-IQA framework for contrast-distorted images by finding that a high contrast image always looks more similar to its enhanced version. Based on this concern, the design philosophy of our blind metric lies in two factors, namely, image similarity, histogram based entropy. Given the input image and the one created through classical histogram equalization (HE), we first concentrate on their appearance. In fact, it is exactly a full-reference IQA problem, and we use classical structural similarity index (SSIM) [25] as the metric. On the other hand, on finding that the histograms of high-contrast and low-contrast images are different, we turn to histograms of the above two images and compute the entropy of original histogram and the enhanced one respectively to reflect the distribution status. Further, we compute the cross entropy to include the interaction between two histograms. Afterward, with the total 5 features, we develop the contrast enhancement based contrast-changed image quality measure (CEIQ) via Support vector regression. Actually, the entropy has already been used for IQA in RCIQM [21] and NIQMC [23]. It is worthwhile to note that CEIQ is different from the previous work. First, the metric RCIQM is not a NR method and needs the histogram of the reference image to compare, while as a NR method, NIQMC compares the input image histogram with the uniformly distributed one. Second, we take advantage of SSIM, which is a benchmark FR-IQA method, in our NR-IQA metric CEIQ because we convert the NR-IQA problem to be a FR-IQA problem by creating a 'reference image' via contrast enhancement. At last, we provide a general framework and any similarity measurement function or contrast enhancement method can be employed in it.

The remainder of this paper is organized as follows. In Section II, we present in details the CEIQ method and demonstrate the high relevance of similarities with image contrast. In Section III, thorough experiments verify the superiority and efficiency of our metric. Section IV concludes this paper.

2. Similarity measurement with equalization

The feature extraction flowchart of the proposed CEIQ is illustrated in Fig. 1. It consists of the following main steps: decolorization, histogram equalization, image similarity, histogram based entropy and cross entropy computation, which are described as follows.

Given an input color image I, on the first step we convert it to a grayscale image I_g for subsequent processing. In particular, the concern here is the choice of the decolorization method. Recently, many methods of color-to-grayscale conversion have been proposed [27-30]. However, most of these methods aim to maximally preserve or even enhance the original color contrast [31]. In our CEIQ framework, our goal is to evaluate the real contrast quality, not to produce the visually-pleasing grayscale result. With this, the original contrast of I should be maintained after decolorization. We produce the grayscale image I_g by YIQ color model:

$$I_g = 0.2989 \times I_{red} + 0.5870 \times I_{green} + 0.1140 \times I_{blue} \tag{1}$$

where I_{red}, I_{green} and I_{blue} denote the RGB channels of I. The YIQ model uses three components: luminance Y and two values I and Q characterizing the chromaticity. This model is used in the American NTSC television norm, and we take the Y channel as the grayscale representation. It should be noted here that the simple method defined in Eq. 1 could not achieve the best grayscale image, but the result image can preserve the original contrast quality with respect to the color image, which is exactly our goal in CEIQ framework. Fig. 2 shows four color images with different contrast quality level selected from CCID2014 database [19], and the quality increases from left to right. Our results using Eq. 1 are shown in the second column. The results via [29] and [30] which are two famous methods for producing visually-pleasing grayscale images, are shown in the third and fourth rows. It bears out the fact that after decolorization, our results reflect very well contrast orders presented in the original images and the gap between the first and fourth images is large, while the quality levels are less discriminable in Fig. 2(c) and Fig. 2(d).

The basis of the proposed method is on the assumption that a high-contrast image is often more similar to its result after contrast enhancement. Our concern here is the choice of contrast enhancement method. Generally, the mainstream enhancement methods can be classified into two categories: histogram-based and Retinex-based [32, 33]. In this paper, the simplicity and automation (means it performs well on almost all types of images without parameter tuning) are two factors to be considered. One key issue is then which method could be used in designing CEIQ? In spite of excessive contrast enhancement, histogram equalization (HE) has proved to be a simple and effective image contrast enhancement technique by flattening and stretching the dynamic range of the image's histogram [32]. With this, we take advantage of the classical HE to achieve the contrast enhancement. To illustrate the results of HE, some original color images I_c with different contrast, their grayscale images I_g and HE results I_e are shown in Fig. 3 (a-c). As stated above, in our CEIQ framework, any improvement of conventional HE based method can also be used. Unlike the contrast enhancement methods which only focus on the appearance of the result image, we care both the original and result images, more

specifically, the similarity of them.

Therefore, given two images I_g and I_e, we continue to extract our contrast-aware features in two aspects.

2.1 Image similarity

Intuitively, the similarity functions used in many existing FR-IQA methods can all be used to compute inter-image similarity. In this paper, we adopt the SSIM, which is calculated by:

$$SSIM(I_g, I_e) = L(I_g, I_e)^\alpha * C(I_g, I_e)^\beta * S(I_g, I_e)^\lambda \tag{2}$$

where constants α, β and λ mediate the relative importance of the three components [25]. *L*, *C* and *S* measure the similarities of luminance, contrast and structure respectively between I_g and I_e. In this work, we follow [25] for the configuration of the parameters. Therefore, we use the similarity of two images defined in Eq. 2 as the first feature S_{ge} in our CEIQ framework.

In our work, we also consider the feature-similarity (FSIM) index [34], which is another excellent FR-IQA method based on SSIM. Its performance will be examined in the section of experimental results.

For the five images shown in Fig. 3, the corresponding mean opinion scores (MOS) increase from left to right, which means that the right one has the highest subjective score given by human. Using Eq. 2, we can easily obtain the corresponding S_{ge} scores: 0.1457, 0.5364, 0.5562, 0.6404 and 0.7735 respectively, which are illustrated in Fig. 4. It can be realized that S_{ge} is monotonically related to the MOS score. Further, we exhibit the scatter plots of MOS/DMOS versus S_{ge} on the whole CCID2014 (including 655 images) and CSIQ (including 116 contrast changed images) database [34] in Fig. 5. Clearly, the score of image similarity shows higher linearity and monotonicity on CCID2014 database, but the performance becomes worse on CSIQ database. So, only one feature is not enough to handle all the contrast distortion models and levels, we should explore more contrast-aware features.

2.2 Histogram based entropy and cross entropy

The second consideration of our proposed metric comes from the histogram. The major reason is that histogram is the indicator of the contrast. We plot the corresponding histograms in Fig. 3(d) and Fig. 3(e). More precisely, entropy is a chief concept in statistics [26], and it represents the amount of information for a random signal by quantifying its average unpredictability. It is reasonable to assume that not only the high-contrast image, but also its contrast enhanced version are of the histogram toward uniform distribution, which stands for the large entropy. Given the histogram h of pixel values, the entropy E is defined by

$$E = -\sum_{i=0}^{b} h(i) \log h(i) \tag{3}$$

where b indicates the value of bins in histogram and $\log(\cdot)$ has base of two. Therefore, given two

histograms h_g and h_e corresponding to the input gray image and the equalized image, we can easily

obtain their entropy E_g and E_e by Eq. 3 as our second and third features.

Further, in our work, we take the relationship between h_g and h_e into consideration by the use of

the cross entropy, which is computed by:

$$E_\mathrm{ge} = -\sum_{i=0}^{b} h_\mathrm{g}(i) \log h_e(i) \tag{4}$$

It should be noted here that the combination of Eq. 3 and Eq. 4 is exactly the classical forma of K-L divergence to estimate the distance between two distributions. However, we take the individual part as one feature in our work to describe the characteristic of one histogram and the interaction between two histograms separately. In the same way, another cross entropy is computed by:

$$E_\mathrm{eg} = -\sum_{i=0}^{b} h_\mathrm{e}(i) \log h_g(i) \tag{5}$$

Thus, we obtain our third and forth features.

Finding a good tradeoff between efficacy and efficiency, we divide the histogram into 128 bins when computing, and we find that the value of bins (such as 64, 128 or 256) has little effect on the performance of CEIQ. In addition, we only take the bins with non-zero values to compute the above four features.

In Fig. 6, two scatter plots of DMOS versus E_e and E_eg on the CSIQ (including 116 contrast

changed images) database are given. From them, we can see that these features perform well than the image similarity on CSIQ database. So, we use the above described five features to represent the contrast quality of the input image.

2.3 The CEIQ metric

For any image, we utilize the image similarity S_ge, histogram based entropy E_g and E_e, cross

entropy E_ge and E_eg to form the feature vector f. We can construct a training set of k images with

their feature vectors and subjective scores $\{(f_1, Q_1), (f_2, Q_2), \cdots, (f_k, Q_k)\}$. A regression function could

be learned to find the mapping function.

The framework is generic enough to allow for the use of any regressor. In our implementation, a SVM regressor (SVR) is adopted. SVR has previously been applied to IQA problems [4, 7, 10, 11, 12, 20, 22, 24]. In this work, we use the LIBSVM package [36] with the linear kernel to implement the SVR. Once the regression model is learned, we use it to estimate the quality of any input image.

3. Experimental Results and Discussions

3.1 Databases and methods for comparison

The source code of our CEIQ has been released at *https://github.com/mtobeiyf/CEIQ*. The proposed method is examined on four contrast distortion related image databases: CID2013 [20], CCID2014 [19], CSIQ [34] and TID2013 [37]. CID2013 and CCID2014 are specifically designed for contrast distortion, including 400 and 655 contrast-changed images generated from 15 natural images respectively. CSIQ is built for various distortion types, among which there are 116 global contrast changed images. TID2013 is a large scale image quality database which contains 3000 images generated from 25 reference with 24 distortion types for each reference. A total number of 240 images which are directly related to contrast distortions (#16 mean shift and #17 contrast change) are utilized here.

We compare the proposed CEIQ with eight state-of-the-art IQA methods: 1) classical FR-IQA methods, including SSIM [25], FSIM [34] and MAD [38]; 2) representative general-purpose NR-IQA methods, including BRISQUE [4] and IL-NIQE [9]; 3) contrast distortion specific NR-IQA methods, including Fang [22], NIQMC [23] and BIQME [24]. It should be stressed here that BRISQUE, FANG, BIQME and our CEIQ are the methods need training, and we put them into a group. Specially, we also consider the score of S_{ge} as one metric to evaluate its performance, and it should be stressed here that this is a training-free metric. The performance of the involved methods is evaluated by three popular criteria computed between predicted scores and subjective scores: Spearman rank order correlation coefficient (SROCC) and Kendall rank order correlation coefficient (KROCC) for prediction monotonicity, Pearson linear correlation coefficient (PLCC) for prediction accuracy. PLCC is computed after the monotonic logistic mapping between objective and subjective scores [39]. A value close to 1 for SROCC, KROCC and PLCC means superior correlation with subjective opinions.

3.2 Overall performance comparison

For the training-free methods, we use all the images in each database to obtain the results. Taking the TID2013 for example, 250 images are all used to compute the coefficients. For the methods require training, we split each database into train and test sets with 80% for training and 20% for testing. The split is conducted according to reference images to guarantee the independency of the image content in training set and test set. This splitting is repeated for 1,000 times and the median results are used to evaluate the final performance. This treatment method is also widely used in training based IQA research, like the experiments in [4, 22, 24].

Table I lists the SROCC, PLCC and KROCC values of examined methods on four databases to show their performance. For better comparing, we divide the NR methods into two groups: training-free and training based. From the results, five conclusions can be derived. First, among training-free methods, even FR ones, our S_{ge} achieves promising results compared to other methods on CID2013, CCID2014 and TID2013 databases. This demonstrate that the image similarity of the input image and the equalized one is really a powerful feature. Second, our CEIQ metric is obviously superior to all the training based models on CCID 2014, CSIQ and TID2013 databases, especially on CSIQ and TID2013 where the CEIQ outperforms others by a significant margin. As to the CID2013 database, the CEIQ is comparable with the best one BIQME (0.8934 vs. 0.9015 with SROCC). Third, apparently, the contrast distortion specific methods outperform the general-purpose methods (IL-NIQE and BRISQUE) by a large extent

because of the special selection of contrast-aware features. Fourth, our CEIQ performs more accurately and consistently than our S_{ge} on all the databases. There are two reasons: 1) entropy based features are added for training step means the model can 'study' the difference between distortion levels; 2) the smaller images are included in the evaluation (20% vs. 100%). Fifth, we surprisingly find that our S_{ge} , which is a training-free metric, even outperforms some training based methods on some databases. For example, the SROCC of S_{ge} on CID2013 is 0.8431, while the result of FANG is 0.7852. The results of

S_{ge} on the four databases can also be found at *https://github.com/mtobeiyf/CEIQ* .

Since our CEIQ is a training based metric, which requires distorted images and their MOS to learn the model, we report the performance of it under different training set sizes. 10%-80% of the images in each database are used for training and the left ones are used for test according to the same method described previously. For each ratio, we compute the median SROCC values among 1000 times on each database, and the results are shown in Fig. 7. This figure witnesses slightly fluctuations from 10% to 80%. In fact, by comparing the results in Table I and Fig. 7, even with only 10% of images for training, the SROCC results of our metric are also quite encouraging compared with other metrics.

In the above experiments, the training and test samples are drawn from the same database. It is expected that the BIQA model learned from one database should be applicable to images in other databases. Therefore, we test the generalization capability of our metric by training it on one database, then testing it on other databases. The SROCC score is used for evaluation, and the results are presented in Fig. 8. Note that when trained on CID2013 or CCID2014 and then applied to other database, our metric deliver excellent performance and outperform other metrics which are trained and test in the same database in Table I. However, it performs poorly when trained on CSIQ or TID2013 database and test on CID2013 and CCID2014 database. The major reason is that the number of images and the contrast distortion levels of CID2013 and CCID 2014 are more than them of the CSIQ and TID2013. For example, there are 45 distorted images generated from one reference image on average in CCID2014 database, while only 4 distorted images corresponding to one reference image are available in CSIQ database.

3.3 Runtime measure

To test the efficiency which is also important in real-world applications, the runtime of involved NR metrics are listed in the Table II. Results are performed on a notebook with Intel Core i7-6700HQ CPU@2.6G Hz and 8GB RAM. The software platform is Matlab R2017a. The computational cost is evaluated with 768×512 RGB image from CCID2014 database. Clearly, our proposed CEIQ owns highest efficiency, followed by BRISQUE and FANG. Compared to the features extracted in BIQME which performs also well in the previous experiments, the major cost of our metric is just the SSIM computation. Hence, the proposed method is quite efficient, outperforming BIQME by a large margin.

3.4 Similarity measurement strategies

As described above, our proposed metric illustrated in Fig. 1 provides a general framework for IQA of contrast-distorted images, and any available method can be employed in it, such as the similarity measurement strategies. Besides the SSIM which we used, in this section, we consider another classical

measurement for inter-image similarity: FSIM [34]. The SROCC results of these methods on CCID2014 database are tabulated in Table III. From the results, it is possible to see that although the FSIM performs better than SSIM in classical FR-IQA problems, its performance is worse than SSIM in our CEIQ. In FSIM, phase congruency (PC) is used as the primary feature [34]. However, PC is contrast invariant, meaning that the images with different contrast distortion level have almost the same scores for PC, which is the main reason of the worse performance of FSIM in our framework.

4   Conclusion

In this paper, we develop a no-reference quality metric CEIQ to assess the quality of contrast changed images using histogram equalization from two aspects: image similarity and histogram based entropy and cross entropy. Experimental results show that the proposed methods are well correlated with subjective evaluations even only few images are used for training, suggesting that the proposed metrics are excellent at handling contrast-distorted images with very low computational cost. Further, CEIQ provides a general framework, and other contrast enhancement methods and image similarity measure metrics can be employed in this framework.

References

[1] W. Lin, C.C. JayKuo, Perceptual visual quality metrics: a survey, Journal of Visual Communication and Image Representation 22 (4) (2011) 297–312.

[2] R. A. Manap, L. Shao, Non-distortion-specific no-reference image quality assessment: a survey, Information Sciences 301 (2015) 141-160.

[3] H. R. Sheikh, A. C. Bovik, L. Cormack, No-reference quality assessment using natural scene statistics: JPEG2000, IEEE Transactions on Image Processing 14 (11) (2005) 1918–1927.

[4] A. Mittal, A. K. Moorthy, A. C. Bovik, No-reference image quality assessment in the spatial domain, IEEE Transactions on Image Processing 21 (12) (2012) 4695–4708.

[5] A. K. Moorthy, A. C. Bovik, Blind image quality assessment: From natural scene statistics to perceptual quality, IEEE Transactions on Image Processing 20 (12) (2011) 3350-3364.

[6] M. A. Saad, A. C. Bovik, C. Charrier, Blind image quality assessment: A natural scene statistics approach in the DCT domain, IEEE Transactions on Image Processing 21 (8) (2012) 3339-3352.

[7] Y. Zhang, D. M. Chandler, An algorithm for no-reference image quality assessment based on log-derivative statistics of natural scenes (2013) [Online]. Available: http://dx.doi.org/10.1117/12.2001342

[8] A. Mittal, R. Soundararajan, A. C. Bovik, Making a "completely blind" image quality analyzer, IEEE Signal Processing Letters 20 (3) (2013) 209-212.

[9] L. Zhang, L. Zhang, A. C. Bovik, A feature-enriched completely blind image quality evaluator, IEEE Transactions on Image Processing 24 (8) (2015) 2579-2591.

[10] D. Lee, K. N. Plataniotis, Toward a no-reference image quality assessment using statistics of perceptual color descriptors, IEEE Transactions on Image Processing 25 (8) (2016) 3875–3889.

[11] J. Yan, W. Zhang, T. Feng, Blind Image Quality Assessment Based on Natural Redundancy Statistics, in: Proceedings of Asian Conference on Computer Vision, 2016, pp. 3-18.

[12] D. Ghadiyaram, A. C. Bovik, Perceptual quality prediction on authentically distorted images using a bag of features approach, Journal of Vision 17 (1) (2016).

[13] W. Hou, X. Gao, D. Tao, X. Li, Blind image quality assessment via deep learning, IEEE Transactions on Neural Networks & Learning Systems 26 (6) (2017) 1275–1286.

[14] H. Tang, N. Joshi, A. Kapoor, Blind image quality assessment using semi-supervised rectifier networks, in: Proceedings of the IEEE Conference on Computer Vision and Pattern Recognition, 2014, pp. 2877-2884.

[15] L. Kang, P. Ye, Convolutional neutral networks for no-reference image quality assessment, in: Proceedings of the IEEE Conference on Computer Vision and Pattern Recognition, 2014, pp.1733-1740.

[16] J. Li, J. Yan, D. Deng, W. Shi, S. Deng, No-reference image quality assessment based on hybrid model, Signal Image & Video Processing 11(6) (2017) 985-992.

[17] S. Bianco, L. Celona, P. Napoletano, R. Schettini, On the Use of Deep Learning for Blind Image Quality Assessment [Online]. Available: https://arxiv.org/abs/1602.05531.

[18] Z. Chen, T. Jiang, Y. Tian, Quality assessment for comparing image enhancement algorithms, in: Proceedings of the IEEE Conference on Computer Vision and Pattern Recognition, 2014, pp. 3003–3010.

[19] K. Gu, G. Zhai, W. Lin, M. Liu, The Analysis of Image Contrast: From Quality Assessment to Automatic Enhancement, IEEE Transactions on Cybernetics 46 (1) (2015) 284-297.

[20] K. Gu, G. Zhai, X. Yang, W. Zhang, M. Liu, Subjective and objective quality assessment for images with contrast change, in: Proceedings of the 20th IEEE Conference on Image Processing, 2013, pp. 383–387.

[21] M. Liu, K. Gu, G. Zhai, J. Zhou, W. Lin, Quality assessment of contrast-altered images, in: Proceedings of the IEEE International Symposium on Circuits and Systems, 2016, pp. 2214-2217.

[22] Y. Fang, K. Ma, Z. Wang, W. Lin, Z. Fang, G. Zhai, No-reference quality assessment of contrast-distorted images based on natural scene statistics, IEEE Signal Processing Letters 22 (7) (2015) 838–842.

[23] K. Gu, W. Lin, G. Zhai, X. Yang, No-Reference Quality Metric of Contrast-Distorted Images Based on Information Maximization, IEEE Transactions on Cybernetics 47 (12) (2017) 4559-4565.

[24] K. Gu, D. Tao, J. Qiao, W. Lin, Learning a No-Reference Quality Assessment Model of Enhanced Images with Big Data, IEEE Transactions on Neural Networks & Learning Systems PP (99) (2017) 1-13.

[25] Z. Wang, A. C. Bovik, H. R. Sheikh, E. P. Simoncelli, Image quality assessment: From error visibility to structural similarity, IEEE Transactions on Image Processing 13 (4) (2004) 600-612.

[26] C. E. Shannon, A mathematical theory of communication, Bell Syst.Tech. J. 27 (1948) 379–423.

[27] M.D. Fairchild, Color Appearance Models, John Wiley & Sons, 2013.

[28] R. Bala, R. Eschbach, Spatial Color-to-Grayscale Transform Preserving Chrominance Edge Information, in: Proceedings of the Color and Imaging Conference, 2004, pp. 82-86.

[29] M. Grundland, N. A. Dodgson, Decolorize: Fast, contrast enhancing, color to grayscale conversion, Pattern Recognition 40 (11) (2007) 2891-2896.

[30] C. Lu, L. Xu, J. Jia, Contrast preserving decolorization, in: Proceedings of the IEEE International Conference on Computational Photography, 2012, pp. 1-7.

[31] K. Ma, T. Zhao, K. Zeng, Z. Wang, Objective Quality Assessment for Color-to-Gray Image Conversion, IEEE Transactions on Image Processing 24 (12) (2015) 4673-4685.

[32] M. Kaur, J. Kaur, J. Kaur, Survey of Contrast Enhancement Techniques based on Histogram Equalization, International Journal of Advanced Computer Science & Applications 2 (7) (2011) 137-141.

[33] H. Yue, J. Yang, X. Sun, F. Wu, C. Hou, Contrast Enhancement Based on Intrinsic Image Decomposition, IEEE Transactions on Image Processing 26 (8) (2017) 3981-3994.

[34] L. Zhang, L. Zhang, X. Mou, D. Zhang, FSIM: a feature similarity index for image quality assessment, IEEE Transactions on Image Processing 20 (8) (2011) 2378-2386.

[35] E. C. Larson, D. M. Chandler, Most apparent distortion: Full reference image quality assessment and the role of strategy, Journal of Electronic Imaging, 19 (1) (2010) 143-153.

[36] C. C. Chang, C. J. Lin, LIBSVM: A Library for Support Vector Machines, http://www.csie.ntu.edu.tw/~cjlin/libsvm/, 2001.

[37] N. Ponomarenko, O. Ieremeiev, V. Lukin, K. Egiazarian, L. Jin, J. Astola, B. Vozel, K. Chehdi, M. Carli, F. Battisti, C.C.J. Kuo, Color image database TID2013: Peculiarities and preliminary results, in: Proceedings of the European Workshop on Visual Information Processing, 2013, pp. 106-111.

[38] E. C. Larson, D. M. Chandler, Most apparent distortion: Full reference image quality assessment and the role of strategy, Journal of Electronic Imaging 19 (1) (2010) 011006.

[39] VQEG, Final report from the video quality experts group on the validation of objective models of video quality assessment, VQEG, 2000.
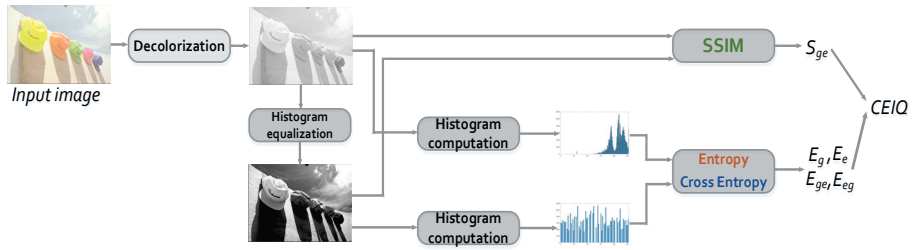
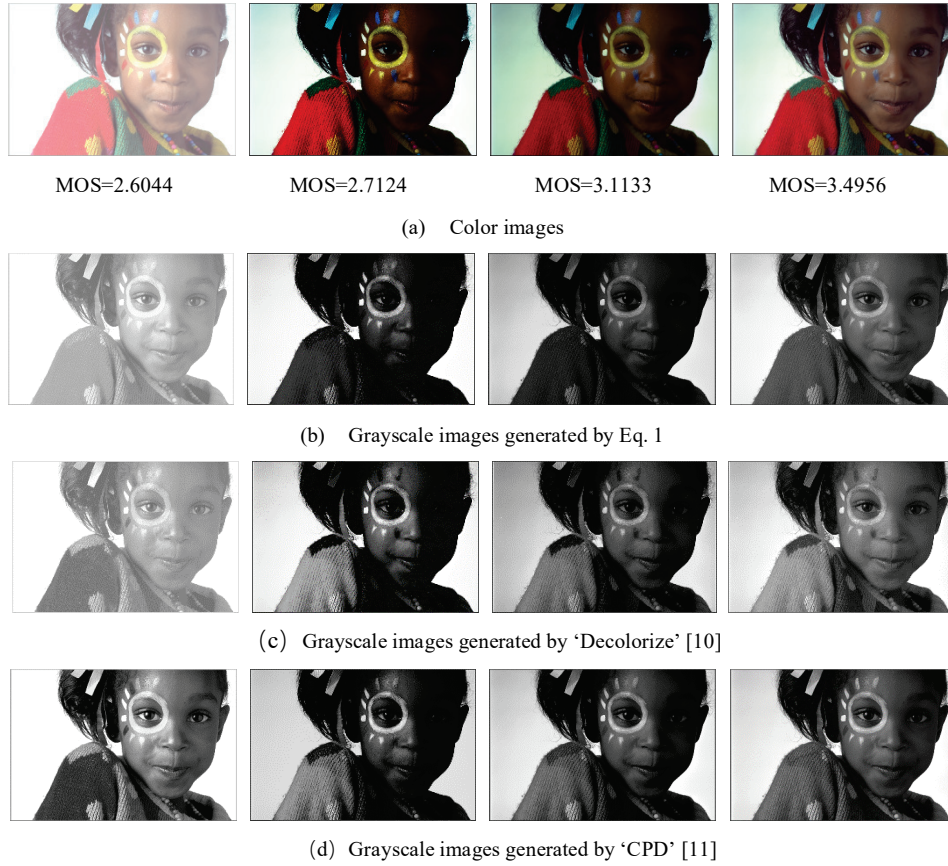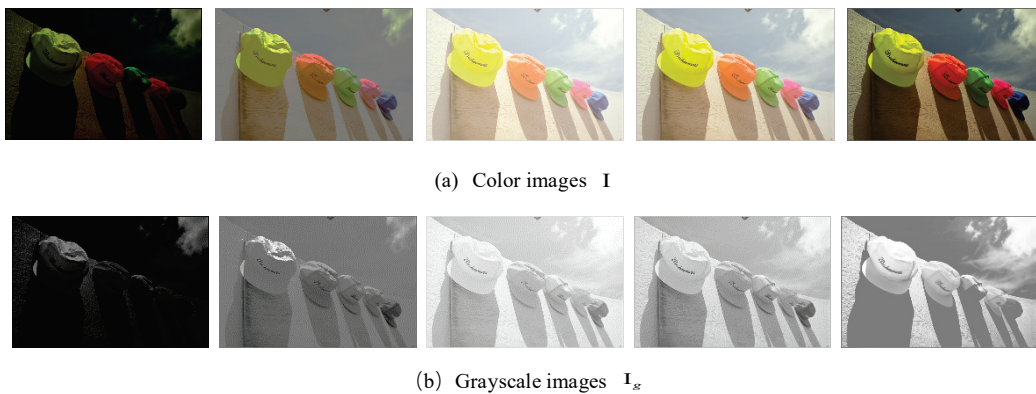Fig. 1. The feature extraction flowchart of our proposed CEIQ algorithm

MOS=2.6044   MOS=2.7124   MOS=3.1133   MOS=3.4956

(a)   Color images

(b)   Grayscale images generated by Eq. 1

(c)   Grayscale images generated by 'Decolorize' [10]

(d) Grayscale images generated by 'CPD' [11]

Fig. 2. Comparison with other decolorization methods

(a) Color images $\mathbf{I}$

(b) Grayscale images $\mathbf{I}_g$

(c) Contrast enhanced images $\mathbf{I}_e$
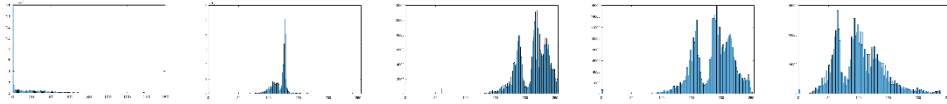
(d) Histogram $\mathbf{h}_g$ of $\mathbf{I}_g$
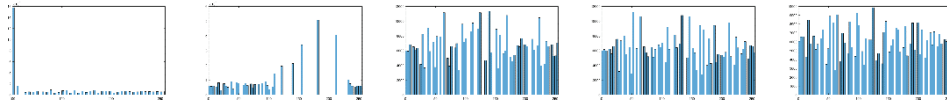
(e) Histogram $\mathbf{h}_e$ of $\mathbf{I}_e$

Fig. 3. The histograms of grayscale images and the contrast enhanced ones using HE.
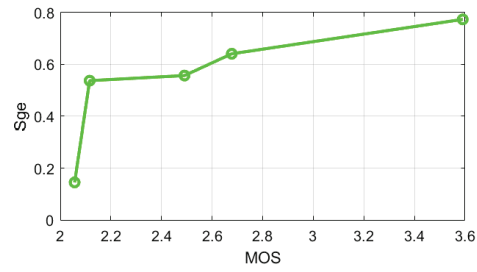

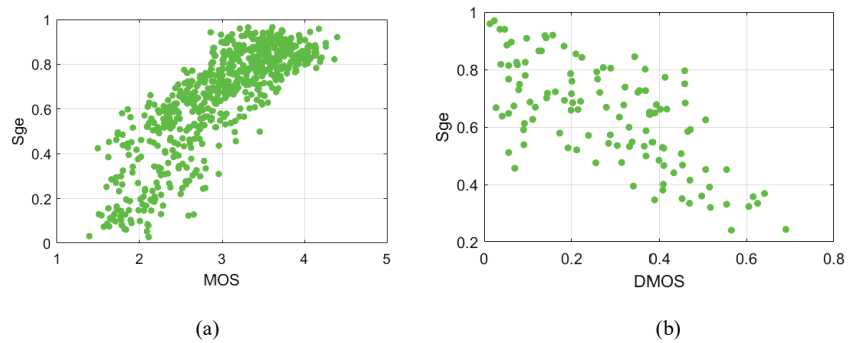Fig. 4. Comparison between S_{ge} and subjective MOS of five images from CCID2014

(a)   (b)

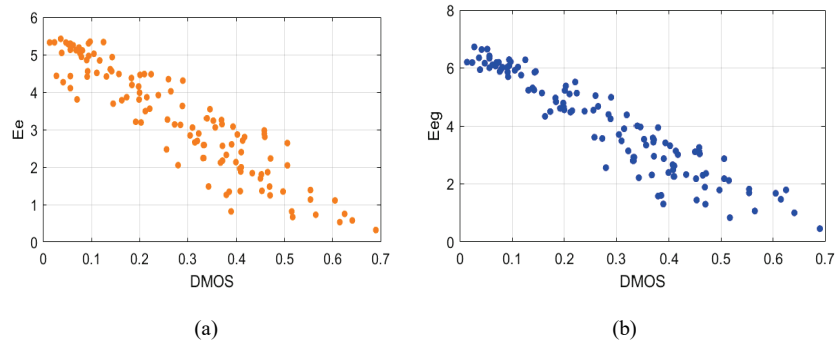Fig. 5. Scatter plots of MOS/DMOS versus S_{ge}. (a) CCID2014 database (b) CSIQ database

Fig. 6. Scatter plots of DMOS versus E_e (a) and E_{eg} (b) on CSIQ database
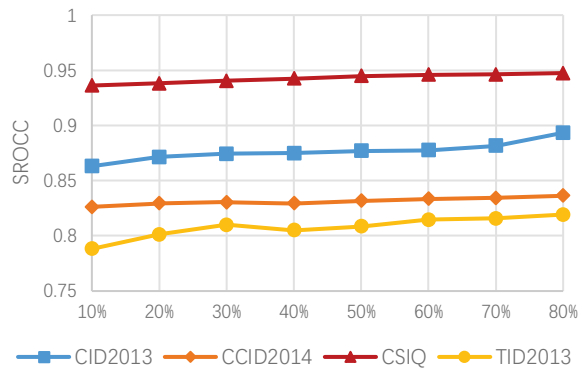

Fig. 7. SROCC with different split ratios on four image databases

(a) Trained on CID2013

(b) Trained on CCID2014

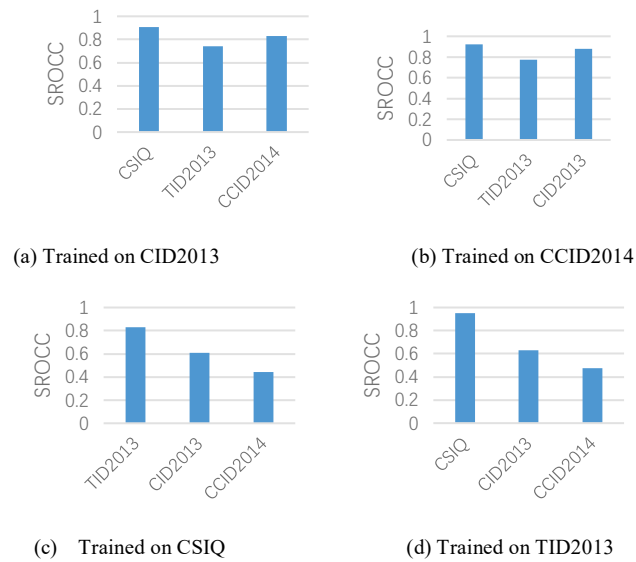(c)   Trained on CSIQ

(d) Trained on TID2013

Fig. 8 Cross-Database performance of our proposed metric

TABLE I

Performance comparison of 10 IQA methods. The top one for each group is highlighted.

Quality Metrics	Type	Training	CSIQ (116 images)			TID2013 (240 images)		
			SROCC	PLCC	KROCC	SROCC	PLCC	KROCC
SSIM	FR	No	0.7397	0.7450	0.5323	**0.4905**	0.5658	0.3432
FSIM	FR	No	**0.9420**	**0.9378**	**0.7883**	0.4413	**0.6819**	**0.3588**
MAD	FR	No	0.9207	0.9321	0.7460	0.3300	0.4077	0.2558
IL-NIQE	NR	No	0.5005	0.5468	0.3510	0.1517	0.2275	0.1030
NIQMC	NR	No	**0.8533**	**0.8747**	**0.6689**	0.6458	**0.7225**	**0.4687**
S_{ge}(Pro.)	NR	No	0.6154	0.7112	0.4483	**0.6491**	0.6029	0.4442
BRISQUE	NR	Yes	0.2539	0.3488	0.1706	0.0551	0.1429	0.0359
FANG	NR	Yes	0.7232	0.6998	0.5178	0.3478	0.4113	0.2291
BIQME	NR	Yes	0.8202	0.8276	0.6501	0.6510	0.7479	0.4783
CEIQ(Pro.)	NR	Yes	**0.9475**	**0.9532**	**0.8182**	**0.8193**	**0.8718**	**0.6302**
Quality Metrics	Type	Training	CID2013 (400 images)			CCID2014 (655 images)		
			SROCC	PLCC	KROCC	SROCC	PLCC	KROCC
SSIM	FR	No	0.8132	0.8072	0.5513	**0.8136**	**0.8256**	**0.6063**
FSIM	FR	No	**0.8486**	**0.8574**	**0.6663**	0.7658	0.8201	0.5707
MAD	FR	No	0.8079	0.8151	0.5912	0.7430	0.7928	0.5458
IL-NIQE	NR	No	0.5273	0.5682	0.3708	0.5121	0.5764	0.3590
NIQMC	NR	No	**0.8668**	**0.8691**	**0.6690**	0.8113	**0.8438**	**0.6052**
S_{ge}(Pro.)	NR	No	0.8431	0.8524	0.6412	**0.8120**	0.8422	**0.6052**
BRISQUE	NR	Yes	0.2552	0.3351	0.1745	0.2123	0.3575	0.1445
FANG	NR	Yes	0.7852	0.7801	0.6035	0.7786	0.8012	0.5711
BIQME	NR	Yes	**0.9015**	**0.8989**	**0.7323**	0.8321	0.8511	**0.6565**
CEIQ(Pro.)	NR	Yes	0.8934	0.8960	0.7085	**0.8363**	**0.8675**	0.6362

TABLE II

Runtime comparison of evaluated NR metrics

Metrics	Number of features	Time (second/image)
IL-NIQE	468	2.331
NIQMC	2	2.213
BRISQUE	36	0.211
FANG	5	0.5831
BIQME	17	0.762
CEIQ	5	0.056

TABLE III

SROCC results of different combination forms in CEIQ

Metrics	SROCC
CEIQ (SSIM)	0.8363
CEIQ (FSIM)	0.8121